

A WIDERÖE PRE-ACCELERATOR FOR THE SUPERHILAC*

1976 Proton Linear Accelerator Conference

J. Staples, J. Alonso, G. Behrsing, D. Clark,
 H. Grunder, M. Olivier, D. Spence, R. Yourd
 Lawrence Berkeley Laboratory
 University of California
 Berkeley, California

NOTICE

This report was prepared as an account of work sponsored by the United States Government. Neither the United States nor the United States Energy Research and Development Administration, nor any of their employees, nor any of their contractors, subcontractors, or their employees, makes any warranty, express or implied, or assumes any legal liability for the accuracy, completeness or usefulness of any information, apparatus, product or process disclosed, or represents that its use would not infringe privately owned rights.

Summary

In 1971 the Bevatron successfully accelerated low-intensity heavy ion beams up to neon to energies of 2.1 GeV/amu. More recently, beams up to argon have been accelerated using the SuperHILAC as an injector to the Bevatron—the Bevalac concept. With increasing scientific interest in high-energy high-intensity beams of heavier ions, plans to upgrade both the Bevatron vacuum system and the SuperHILAC ion sources and injectors have been formulated. A proposed new pre-accelerator based on an air-insulated Cockcroft-Walton and a Wideröe linac is presented.

The Wideröe linac uses the design concepts established at UNILAC¹, modified for our frequency and energy requirements. U^{7+} from the ion source is accelerated from 12 keV/amu to 113 keV/amu and stripped to a mean charge state acceptable to the first tank of the SuperHILAC. The expected intensity improvement over the present pressurized injector is a factor of 100 at the highest masses.

The physical modeling of the Wideröe linac structure will be kept to a minimum. Computer models predicting the characteristics of the structure have improved to the point where the probability of satisfactory performance is high.

Introduction

The first tank of the SuperHILAC requires a particle velocity $B = 0.0154$ (corresponding to energy of 0.1125 MeV per nucleon) and a charge to mass ratio of 0.046 or larger. Experience with the two existing injectors provides substantial help in defining the general requirements of a new high-intensity injector for beams above mass 86. The necessary performance indicates an air-insulated Cockcroft-Walton as the pre-accelerator for easy source accessibility and overall reliability followed by a Wideröe linac. The beam will then be stripped to a higher charge state before being injected into the SuperHILAC. A Wideröe accelerator operating successfully at the UNILAC facility in Darmstadt, Germany, serves as the model of our proposed accelerator.

Pre-Accelerator

The ion source, located in the terminal of a

¹K. Kaspar, GSI Report 73-10, Darmstadt (1973).

*This report was done with support from the United States Energy Research and Development Administration. Any conclusions or opinions expressed in this report represent solely those of the author(s) and not necessarily those of The Regents of the University of California, the Lawrence Berkeley Laboratory or the United States Energy Research and Development Administration.

conventional 400 kV Cockcroft-Walton pre-accelerator, will be a high-power Penning Ion Gauge (PIG) source. It will produce ions up to mass 140 with a charge-to-mass ratio $q/m \geq 0.046$, which need not be stripped before injection into the SuperHILAC. This source will also provide U^{7+} ions ($q/m = 0.029$, which will be stripped to U^{11+} after the injector linac).

Isotope separation is accomplished in the transport line from the Cockcroft-Walton to the Wideröe linac by magnetic analysis. The ion beam is bent through a total angle of 90 degrees, and a single isotope is selected with a mass discrimination of 1 part in 250.

Table 1 - Parameters of third injector

Cockcroft-Walton Pre-accelerator:

Terminal voltage	$220 U^{7+}$	400 kV
Average currents	15 mA	
Regulation	0.1%	
Power available, terminal	50 kW	
Terminal volume	35 m ³	

Ion Sources:

Type	Radial Extraction PIG
$220 U$ charge state	$7+$
$220 U$ flux	$7 \times 10^{14}/\text{sec}$
Arc voltage, peak	1 kV
Arc current, peak	15 A
Duty factor	33%

Wideröe Structure:

Length	4.45 m
Input energy	11.8 keV/amu
Output energy	112.6 keV/amu
Magnet power requirement	15 kW dc
RF power requirement	50 kW peak RF

Stripper:

Type	Fluorocarbon vapor
Efficiency	15% for U^{11+}

General Wideröe Parameters

The accelerator design is based on the requirement that U^{7+} from a 400 kV Cockcroft-Walton is to be accelerated to 113 keV/amu, the energy required for injection, after stripping, into the first tank of the SuperHILAC. Limitations on attainable quadrupole strength in the first few drift tubes have influenced the choice of structure and operating frequency. The basic structure parameters are shown in Table 2.

The total voltage integral of this structure for a synchronous particle is 3.44 MV. The operating frequency is 23.4 MHz, one-third of the SuperHILAC frequency, thus filling every third r.f. bucket of the SuperHILAC. The integrated quadrupole

field of 55 kg requires that the quadrupoles be at least 7 cm long at the beginning of the Wideröe, so we adopt a structure in which the length of the cells alternates between $3\lambda/2$ and $3\lambda/2$, with the longer drift tubes containing quadrupole focusing elements in a FODO sequence.

The field in the accelerating gaps is kept to less than 56 kV/cm by tapering the g/L and gap voltage along the beam axis. In this way satisfactory beam dynamics can be maintained with conservative voltage and power levels.

Table 2

Basic Structure Characteristics

Particle Characteristics

T_{inj}	11.76 KeV/amu
T_{out}	113 KeV/amu
e/m	.0294

Structure

f	23.4 MHz
number of drift tubes	35
Line voltage	100 - 250 kV
Length	4.45 m

Accelerating Gaps

g/B	.65 - .45
gap field	46 - 56 kV/cm
Aperture radius	1.25 - 1.75 cm
TTF	.5 - .84

Focusing

Number of quads	17
Sequence	FODO
dB/dr	7.6 - 2.3 kg/cm

Acceptances

Transverse area	$15\pi - 22\pi$ cm ²
Energy Acceptance	± 2 keV/amu
Phase Acceptance	$\pm 30^\circ$

The detailed drift tube schedule is shown in Table 3. There are 33 drift tubes, plus two half drift tubes on the end flanges. Sixteen of the drift tubes, containing focusing quadrupoles with field gradients up to 7.6 kg/cm, are suspended from the outer wall of the tank, allowing relative ease in providing power, cooling and alignment. The other 17 short drift tubes are mounted on the inner coaxial conductor and do not contain quadrupoles. However, the support stems of all the drift tubes dissipate considerable r.f. power and are liquid cooled.

The eccentric center conductor is mounted on three stubs, which provide mechanical support and a path for the cooling lines. The r.f. drive loop will be contained in the third support stub. Each stub will have a movable shorting plate which controls the gap voltage profile and resonant frequency of the structure. The physical characteristics of the stub lines and the power dissipation in various accelerator components are shown in Table 4.

Table 3

Cell No	Energy (MeV/amu)	L _{tot} (cm)	V _{gap} (kV)	L _{gap} (cm)	L _{dt} (cm)	TTF
0	.012	0				
1	.013	6.5	106.0	2.13	1.16	.495
2	.015	13.6	123.9	2.28	8.58	.648
3	.017	20.9	128.7	2.30	1.45	.568
4	.019	29.0	128.0	2.45	9.75	.685
5	.021	37.2	126.3	2.47	1.73	.624
6	.023	46.1	126.1	2.60	10.89	.717
7	.025	55.2	125.7	2.61	2.02	.668
8	.028	64.9	126.1	2.73	12.00	.743
9	.030	74.8	127.0	2.73	2.31	.725
10	.032	85.3	127.0	2.84	13.08	.766
11	.035	96.0	125.8	2.85	2.59	.737
12	.037	107.3	125.0	2.95	14.10	.784
13	.039	118.7	127.2	2.95	2.86	.763
14	.042	130.7	128.2	3.04	15.11	.798
15	.044	142.9	135.7	3.05	3.12	.691
16	.047	155.6	137.9	3.13	16.05	.750
17	.049	168.5	144.2	3.14	3.38	.715
18	.052	181.9	146.3	3.23	17.02	.764
19	.055	195.5	156.1	3.24	3.65	.737
20	.058	209.7	159.1	3.33	18.04	.778
21	.061	224.0	167.1	3.34	3.92	.758
22	.065	238.9	169.1	3.44	19.08	.790
23	.068	254.0	175.8	3.46	4.19	.778
24	.071	269.7	178.8	3.56	20.14	.800
25	.075	285.1	187.3	3.59	4.46	.792
26	.079	302.2	190.9	3.70	21.21	.809
27	.083	318.9	198.9	3.74	4.71	.806
28	.087	336.2	200.7	3.86	22.28	.817
29	.091	353.8	205.7	3.91	4.95	.818
30	.095	371.9	208.1	4.05	23.33	.824
31	.100	390.3	212.7	4.10	5.16	.829
32	.104	409.3	213.1	4.26	24.35	.828
33	.109	428.5	213.9	4.32	5.34	.835
34	.113	448.3	196.8	4.48		.831

Table 4

Stub Line Dimensions and Power Dissipation

Stub	Distance from front of line	Length	Z _s	Power Dissipation
1	50 cm	70 cm	70 ohms	3.1 KW
2	170 cm	70 cm	70 ohms	5.1 KW
3	340 cm	100 cm	70 ohms	7.1 KW

Power Dissipation*

All drift tubes and stems	5.0 KW
Drift tube line	2.9 KW
Tank wall	0.4 KW
Stub line center conductors	8.9 KW
Stub line shorting plungers	3.7 KW
Stub line outer walls	2.7 KW

Total Power Dissipation 23.6 KW

* 50% duty factor, includes 10% joint losses

Modeling of the Structure

In designing this structure, a knowledge of voltage distribution along the beam axis is necessary before the drift tube table can be generated. But because of the accelerator's required electrical characteristics, the drift tube properties

themselves affect the voltage distribution. Therefore, any modeling procedure is by necessity an interactive process.

We can make reasonable initial guesses of the voltage distribution and from it derive a drift tube schedule. Reliable computer codes, such as PARMILA², can then investigate beam dynamics for various types of random and systematic errors in the structure. The drift tube properties of our machine have been designed using such a computer code, suitably modified to deal with a Wideröe structure.

However, methods to establish the electrical characteristics of resonant-line type structures are not as well established. The UNILAC Wideröe, upon which our structure is based, went through an extensive modeling procedure before its actual construction. A small, very simplified electrical analogue was built to provide transmission line model data for computer code which then modeled the actual machine. The computer generated model was built at half-scale, and the performance discrepancies between the computer predictions and physical model operation were accounted for in the final design of the actual accelerator.

We have written a computer code to model the electrical characteristics of the present structure, using the same distributed transmission line algorithm as the UNILAC code. The code predicts the resonant frequency, the voltage, current and power distribution, and the sensitivity to parameter changes. The types of discrepancies between the UNILAC half-scale model and the code predictions have been taken into account in the present design.

In our code, the structure is modeled as a dispersive transmission line with three shunt stub lines and a capacitance at each end. The effects of the drift tubes and supports, which were determined in the one-eight constant-velocity model structures³ are included as dispersion in the model transmission line.

The code predicts the voltage distribution on the transmission line itself. Two models have been used to calculate the effect of the stem inductance and inter-gap capacitance, which increase the gap voltage over the line voltage. Analyzing this effect with a simple independent series resonant model and with a second model in which all drift tubes are capacitively coupled, both predict this effect in good agreement with UNILAC data, including the partial suppression of voltage increase at the two end gaps. Another effect observed but not predicted by these models is the anomalously large gap voltage in the vicinity of the three support stub lines. This effect is due to the mutual inductance between the stub lines, which carry a large r.f. current, and the nearby drift tube stems. Rather than calculate this, a function was fitted to the published UNILAC data in the form of $\Delta V_{\text{gap}} = I_{\text{stub}} M(z)$, where $M(z)$ is the mutual inductance between a stub line and a drift tube stem separated by distance z . This function is shown in Figure 1.

²Swenson & Stovall, MP-30 (1969) and Swenson HP-3/DAS-1 (1967 LASL).

³K. Kaspar.

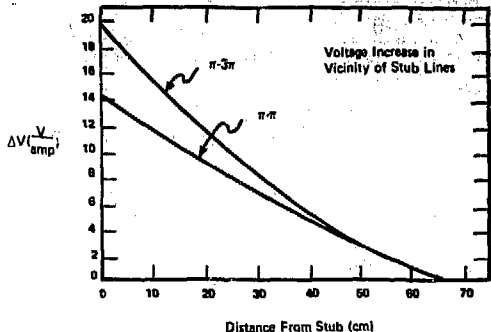


Figure 1

The PARMILA beam dynamics code establishes upper limits of the various types of structure errors. Errors which must be kept small are those such as scatter in the quadrupole position. However, the beam seems to be relatively tolerant of reasonable errors in the accelerating voltage distribution, the quantity most uncertain in the modeling of the electrical structure. With the UNILAC accelerator, the discrepancies between the predicted and the physically modeled structure were corrected by moving the length of one stub line and adjusting the position of the shorting plunger on the stubs, and slightly modifying the drift tube schedule.

We have also extensively studied the sensitivity of the voltage distribution to modifications in stub positions and lengths in our Wideröe. In turn, the sensitivity of the beam dynamics to these changes in voltage distribution has also been examined. We conclude that beam dynamics are essentially unaffected by the maximum structure changes necessary to correct for the discrepancies expected in our computer modeling.

The outcome of these various electrical, dynamics and structure modeling procedures is that we feel that we can predict our total structure with sufficient accuracy that construction of a physical model is unnecessary. In the event that a longitudinal translation of a stub line is required after construction, the flange design permits an off-set. The stub line will be eccentric for a small part of its length but the added equivalent capacitance can be compensated for with the shorting plate.

Wideröe Linac Construction

The tank will be fabricated by the same method as the SuperHILAC, and the tank wall cooling will be by means of extruded aluminum tubes compressed around the perimeter. The three stub lines will be built and attached to the main tank by coupling flange joints, which will permit small longitudinal adjustments. The various Wideröe linac components are identified on Figure 2 and the entire system shown in Figure 3.

The required quadrupole strengths, apertures and drift tube dimensions are nearly identical to one of the groups of magnets in the SuperHILAC. The tape-wound coils in the outer drift tubes are fabricated from copper strip conductor and machined to provide

pole tip openings". The magnet yoke serves as the out member of these drift tubes. Each outer drift tube will be supported and adjusted from a single vertical stem which contains both the coolant passages and magnet power leads. The drift tube will be flooded with liquid freon, to cool the magnet coil and the drift tube shells and stems.

The installed r.f. power is 100 kW; the peak power requirement for U^{7+} is approximately 50 kW.

Wideröe-HILAC Transport Line

The longitudinal matching is achieved by two-double-gap line bunchers operating at 23.4 MHz. The first buncher, located 2.4 meters from the end of the Wideröe, reduces the energy spread of the beam, thereby arresting bunch growth. This cavity will also be used to provide an energy trim to the beam to compensate for losses in the stripper. The second buncher, located 2.4 meters from the Super-HILAC first gap, matches the beam to the longitudinal acceptance of the SuperHILAC by compressing the bunch length.

The transverse matching is accomplished by quadrupole triplets near the Wideröe exit and Super-HILAC entrance and by a pair of doublets near the midpoint of the transfer line.

Stripping

The U^{7+} ions emerging from the Wideröe must be stripped to a charge state of at least $11+$ to be accepted by the SuperHILAC first tank. Stripping is accomplished by passing the beam through either a gas or a thin foil.

Foil stripping produces higher charge states, but the best foils available with present day technology are in danger of being destroyed by high-intensity low energy heavy ion beams. A recent test with 4.5 MeV argon ions from our 2.5 MV Dynamitron injector passing through $5 \mu\text{g}/\text{cm}^2$ carbon foils indicated a 20 minute life-time for ion current densities of 70 particles $\mu\text{amp}/\text{cm}^2$, a fairly typical current expected from the new injector. Such measurements indicate that foil stripping is possible in many applications. Gas stripping produces lower equilibrium charge states, but has no life-time problems and no limits allowed beam currents. Research with very heavy fluorocarbon vapors⁵ has shown a higher charge distribution than for other gases, with adequate fractions of the charge states present for acceleration by the SuperHILAC.

Appendix

The distributed transmission line model, due to Kaspar⁶, with some modifications, is described here.

For a circuit consisting of 4-terminal series admittances Y_S and parallel admittances Y_P , the voltage and current at the output of the network is given by:

⁴R. Main, R. Yourd, Edge Cooled Tape Magnet Coils for High Density Applications, Lawrence Berkeley Laboratory, LBL-1222, October 1972.

⁵D.A. Eastham et al., NIM 133, p. 157 (1976).

⁶K. Kaspar, GSI, 73-10

$$\begin{bmatrix} V_0 \\ I_0 \end{bmatrix} = M \begin{bmatrix} V_1 \\ I_1 \end{bmatrix}$$

where:

$$M_{\text{series}} = \begin{bmatrix} 1 & Y_S \\ 0 & 1 \end{bmatrix}$$

$$M_{\text{parallel}} = \begin{bmatrix} 1 & 0 \\ -Y_P & 1 \end{bmatrix}$$

A transmission line with characteristic impedance Z_C and phase length θ is represented by:

$$M_{\text{line}} = \begin{bmatrix} \cos \theta & -Z_C \sin \theta \\ -Z_C \sin \theta & \cos \theta \end{bmatrix}$$

In a lossless system where all the admittances are purely reactive, we will consider the voltages everywhere real and the current everywhere imaginary.

Separating the real and the imaginary parts of the matrices, and taking their magnitude, we establish a new set of matrices describing the reactive components which are similar, but not identical, to the above matrices:

$$M_{\text{line}} = \begin{bmatrix} \cos \theta & -Z_C \sin \theta \\ \frac{1}{Z_C} \sin \theta & \cos \theta \end{bmatrix}$$

$$M_{\text{shunt cap}} = \begin{bmatrix} 1 & 0 \\ 0 & C_1 \end{bmatrix}$$

$$M_{\text{stub}} = \begin{bmatrix} 1 & 0 \\ -1 & \frac{1}{Z_C \sin \theta} \end{bmatrix}$$

Voltage and current at any point in the structure is given by:

$$V_n = U_0 \cdot M_{1,1}$$

$$I_n = U_0 \cdot M_{2,1}$$

Where M is the product matrix of all elements from the beginning of the structure up to point n and U_0 is a normalization factor. Resonance in the structure is attained when $M_{2,1}$ for the entire structure vanishes, as the admittance at that point is zero (there is no more structure, therefore, no current flows from the last node).

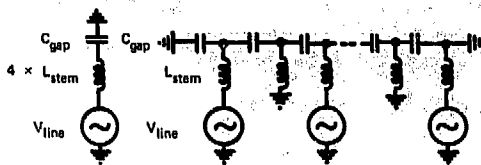
The parameters Z_C and θ describing the transmission line are functions of position along the line and are tabulated by Kaspar. Other quantities needed for calculation of the inter-gap voltage are also tabulated.

Two models have been used to calculate the inter-gap voltages. The first one considers the gap to be the capacitance in a series circuit. This model, Figure 4a, with the inductances of the end stems $2-L$ stem⁷ gives reasonable results.

Another more complex model, Figure 4b, where the drift tubes are capacitively coupled, gives similar results: The difference equation describing this model is

$$-v_{i+1} + \left(2 - \frac{\omega_0^2}{\omega^2}\right) v_i - v_{i-1} = -\frac{\omega_0^2}{\omega^2} v_i$$

where the even V_i are zero and ω_0 is the average resonant frequency of the stem inductance and the inter-gap capacitance.



XBL768-3356

Figure 4a

Figure 4b

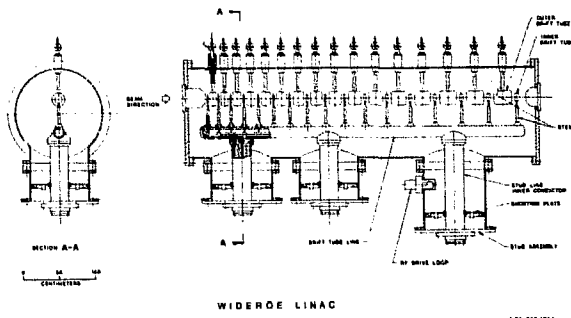


Figure 2

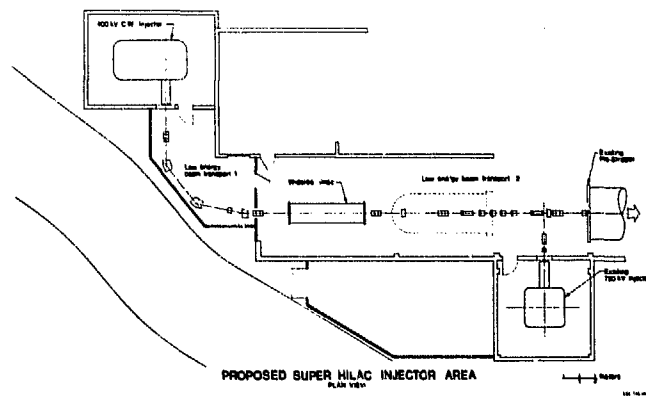


Figure 3